JACC: BASIC TO TRANSLATIONAL SCIENCE VOL. 6, NO. 12, 2021

PRECLINICAL RESEARCH

Rivaroxaban, a Direct Oral Factor Xa Inhibitor, Attenuates Atherosclerosis by Alleviating Factor Xa–PAR2-Mediated Autophagy Suppression

Yusuke Ito, MD, PhD,[a,b] Yasuhiro Maejima, MD, PhD,[a] Shun Nakagama, MD,[a] Yuka Shiheido-Watanabe, DDS, PhD,[a] Natsuko Tamura, MD, PhD,[a] Tetsuo Sasano, MD, PhD[a]

VISUAL ABSTRACT

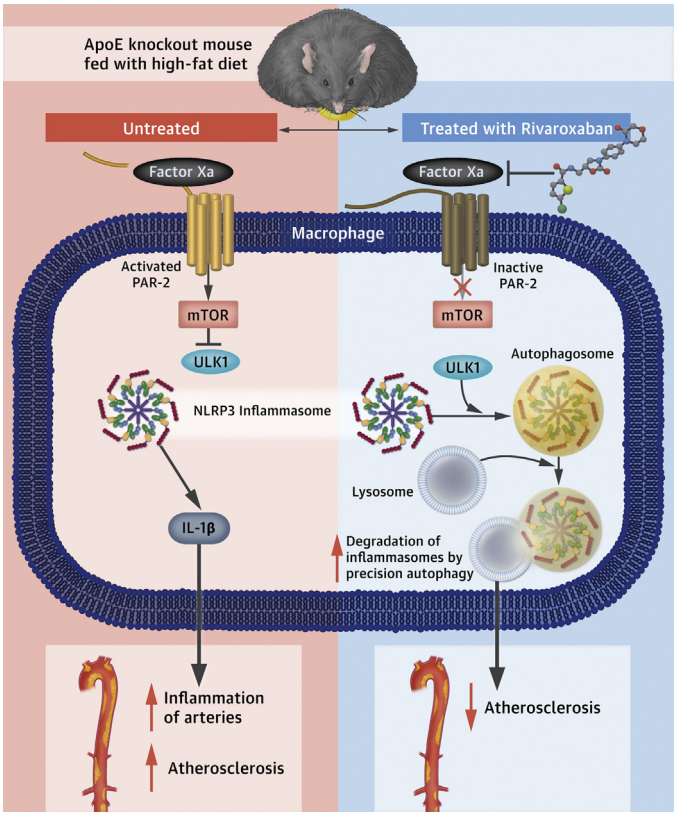

Ito, Y. et al. J Am Coll Cardiol Basic Trans Science. 2021;6(12):964–980.

HIGHLIGHTS

- **An appropriate dose of RIV to inhibit the activity of factor Xa significantly suppressed the atherosclerotic area in the aorta of HFD-fed ApoE$^{-/-}$ mice.**
- **Macrophage autophagy induced by 7KC administration was suppressed by the presence of factor Xa, resulting in the acceleration of inflammasome formation through the PAR2-mediated pathway.**
- **The administration of CQ, an autophagy inhibitor, to HFD-fed ApoE$^{-/-}$/PAR2 knockout bigenic mice significantly aggravated atherosclerosis in the aorta compared with untreated mice.**

From the [a]Department of Cardiovascular Medicine, Tokyo Medical and Dental University, Tokyo, Japan; and the [b]Department of Cardiovascular Medicine, Tokyo Kyosai Hospital, Tokyo, Japan.
The authors attest they are in compliance with human studies committees and animal welfare regulations of the authors' institutions and Food and Drug Administration guidelines, including patient consent where appropriate. For more information, visit the Author Center.

Manuscript received June 1, 2021; revised manuscript received September 30, 2021, accepted September 30, 2021.

ISSN 2452-302X https://doi.org/10.1016/j.jacbts.2021.09.010

SUMMARY

The authors showed a mechanism for attenuating atherosclerosis by directly administering an oral factor Xa inhibitor (ie, rivaroxaban [RIV]). The autophagy activity of macrophages was significantly suppressed by factor Xa and was alleviated by the administration of RIV. However, factor Xa failed to inhibit 7-ketocholesterol–induced autophagy and inflammasome activation in protease-activated receptor 2 (PAR2) knockout macrophages. The atherosclerotic area of apolipoprotein E knockout mice was significantly reduced by the genetic ablation of PAR2, which was partially reversed by chloroquine. Thus, the authors found that RIV attenuates atherogenesis by inhibiting the factor Xa–PAR2-mediated suppression of macrophage autophagy and abrogating inflammasome activity. (J Am Coll Cardiol Basic Trans Science 2021;6:964–980)

ABBREVIATIONS AND ACRONYMS

7KC = 7-ketocholesterol

ApoE$^{-/-}$ = apolipoprotein E deficient

BSA = bovine serum albumin

CAD = coronary artery disease

CQ = chloroquine

ELISA = enzyme-linked immunosorbent assay

FBS = fetal bovine serum

HFD = high-fat diet

IL = interleukin

mTOR = mammalian target of rapamycin

NLRP3 = NLR family pyrin domain containing 3

PAR2 = protease-activated receptor 2

PB = phosphate buffer

PBS = phosphate-buffered saline

PLA = proximity ligation assay

PT = prothrombin time

WT = wild type

Atherosclerosis is a chronic arterial disease that may have critical consequences, such as acute coronary syndrome and stroke, which are the major causes of death worldwide (1). Treatments for atherosclerosis are currently based on drug therapy, including lipid-lowering agents, antihypertensive drugs, and agents for the treatment of diabetes mellitus. However, the maximum efficacy of these therapies for inhibiting the formation or progression of atherosclerotic lesions is only 30% to 40% (2). Thus, novel strategies for ameliorating atherosclerotic lesions are eagerly anticipated.

Factor Xa is a protease that initiates the final common pathway of the coagulation cascade and results in thrombin formation (3). Rivaroxaban (RIV), a selective inhibitor of factor Xa, is widely used as a potent anticoagulant agent for preventing cerebral embolism in patients with atrial fibrillation and pulmonary thromboembolism in patients with deep vein thrombosis (4–9). In addition, large-scale clinical trials (ATLAS ACS 2-TIMI 51 [Acute Coronary Syndrome-Thrombolysis in Myocardial Infarction 51] study and COMPASS [Cardiovascular Outcomes for People using Anticoagulation Strategies] trial) have shown that RIV could be effective for reducing the risk of death from coronary artery diseases (CADs) (10,11), suggesting that RIV plays a significant role in suppressing the progression of atherosclerosis and the rupture of unstable atherosclerotic lesions. Several previous preclinical studies clearly demonstrated that RIV alleviated the progression of atherosclerotic lesions and promoted plaque stability in apolipoprotein E-deficient (ApoE$^{-/-}$) mice (12–14). However, details with regard to the mechanism by which RIV negatively regulates the progression of atherosclerotic lesions and plaque instability remain unknown.

Accumulating evidence suggests that coagulation factors, such as factor Xa, enhance the exacerbation of atherosclerotic lesions through indirect involvement in thrombus formation via receptor-mediated signaling pathways, such as protease-activated receptors (15). Protease-activated receptor 2 (PAR2), which is activated by factor Xa, facilitates vascular inflammation (16) by inhibiting Akt kinase activity (17), promoting mammalian target of rapamycin (mTOR) activity (18), and inducing lymphocyte migration and adhesion to endothelial cells (19), thereby improving atherogenesis (20). Recent investigations have demonstrated that autophagy dysfunction mediated by inflammation in vascular cells promotes atherosclerosis (21,22). Autophagy, a self-degradation system by which damaged organelles are delivered to and degraded in the lysosome (23), is known to be inhibited by the down-regulation of Akt or the up-regulation of mTOR. These observations led us to hypothesize that factor Xa–mediated PAR2 activation may play a critical role in the progression of atherosclerosis, partially through the down-regulation of the autophagy machinery.

In the present study, we focused on exploring the detailed mechanism whereby RIV attenuates atherosclerosis progression and promotes the stability of advanced atherosclerotic lesions in hyperlipidemic ApoE$^{-/-}$ mice.

METHODS

EXPERIMENTAL ANIMALS. We used 8 12-week-old male mice of C57BL/6J wild type (WT) (CLEA Japan), ApoE$^{-/-}$ (#002052), and PAR2$^{-/-}$ (#004993) (Jackson Laboratory). To generate ApoE$^{-/-}$/PAR2$^{-/-}$ bigenic mice, ApoE$^{-/-}$ mice were intercrossed with PAR2$^{-/-}$ mice. These animals were housed in a pathogen-free animal care facility under standard laboratory conditions (27°C, 40%–60% humidity, 12-hour light/

FIGURE 1 Pharmacologic Effects of Polyethylene Glycol 400-Aggregated RIV Administration on Plasma Concentration, Plasma Factor Xa Levels, and PT in Mice

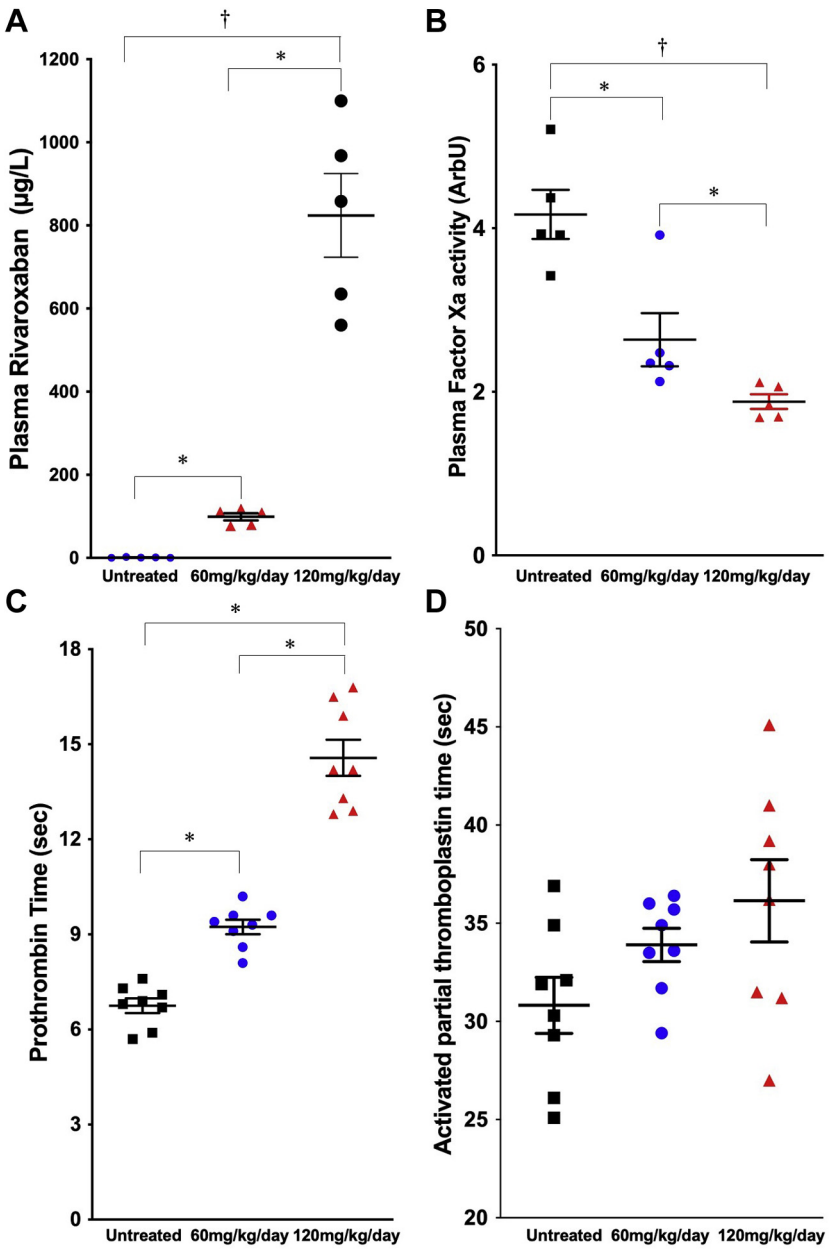

(A) Plasma concentration of rivaroxaban (RIV) in response to 60- or 120-mg/kg/d administration of RIV. *$P < 0.05$, †$P < 0.01$ (n = 5). **(B)** Quantitative analysis of plasma factor Xa activity in mice administered with the indicated dosage of RIV. *$P < 0.05$, †$P < 0.01$ (n = 5). **(C)** Quantitative analysis of prothrombin time in mice administered with the indicated dosage of RIV. *$P < 0.05$ (n = 8). **(D)** Quantitative analysis of activated partial thromboplastin time in mice administered with the indicated dosage of RIV (n = 8). All data are expressed as dot plots, with lines indicating the mean ± standard error of the mean.

12-hour dark cycle) and allowed full access to standard rodent chow (CLEA Japan) and fresh water. ApoE$^{-/-}$ mice and ApoE$^{-/-}$/PAR2$^{-/-}$ bigenic mice were fed a Western-type high-fat diet (HFD) containing 21% pork lard and 0.15% cholesterol (HFD 32, CLEA Japan) for 20 weeks with daily oral gavage administration of 120 mg/kg polyethylene glycol 400-aggregated RIV (Bayer). All animal care and experimental

FIGURE 2 **Administration of RIV Markedly Reduces Atherosclerotic Plaques in HFD-Fed ApoE$^{-/-}$ Mice**

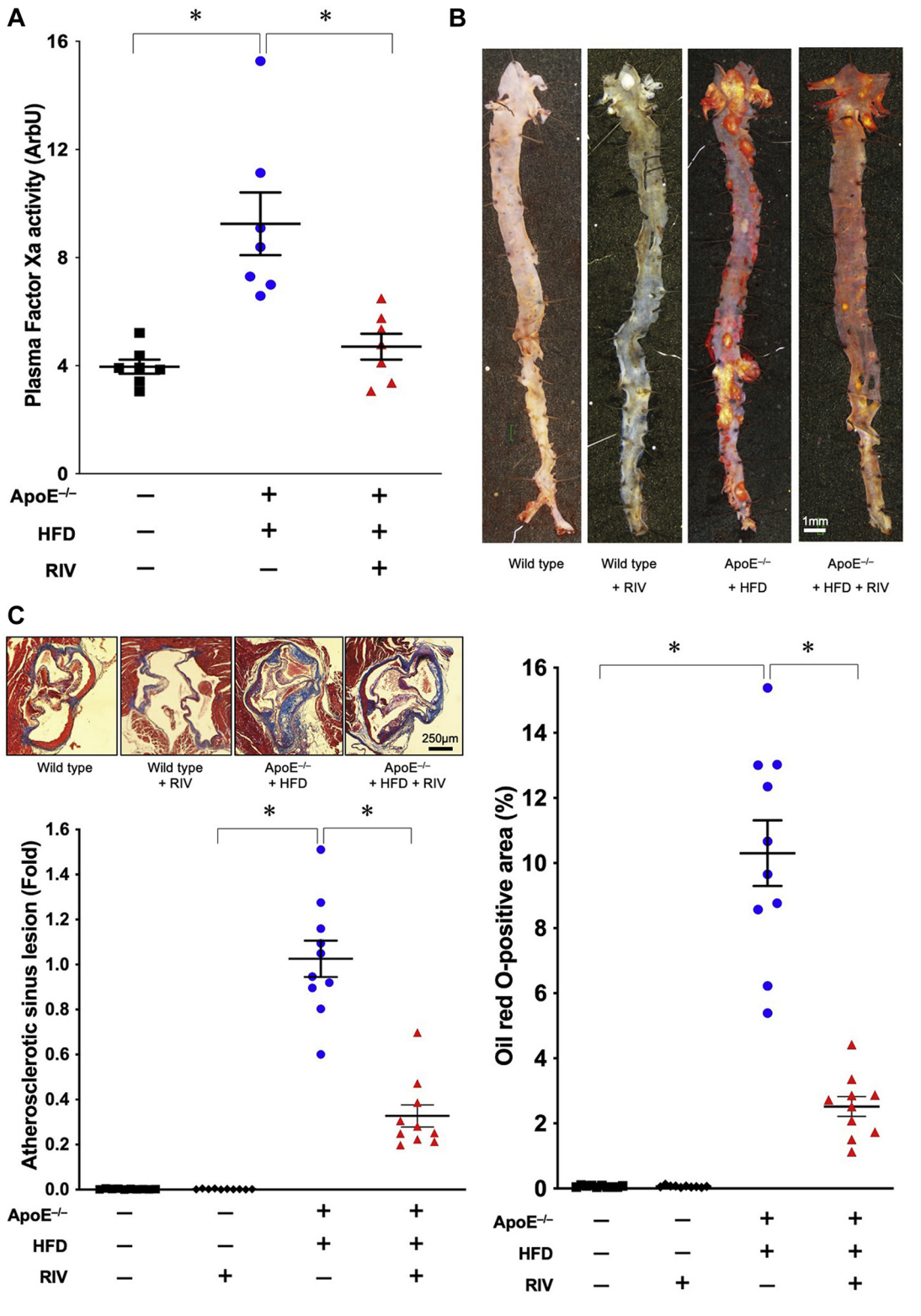

Continued on the next page

procedures were approved by the Tokyo Medical and Dental University Guide for the Care and Use of Laboratory Animals (permit number: A2020-033C2) and the Guide for the Care and Use of Laboratory Animals published by the U.S. National Institutes of Health.

CELL CULTURE. RAW264.7 cells (American Type Culture Collection: TIB-71, lot no. 61524889) were cultured in RPMI-1641 (Sigma-Aldrich) supplemented with 10% fetal bovine serum (FBS) and 1% penicillin/streptomycin. All cells were maintained at 37°C in a 5% CO_2 incubator. For the isolation of peritoneal macrophages, mice were intraperitoneally injected with 1.5 mL 3% Brewer thioglycollate broth (Sigma-Aldrich). After 6 days, primary macrophages were collected from sacrificed animals by peritoneal lavage using 10 mL ice-cold RPMI-1641 supplemented with 10% FBS, 1 U/mL heparin, and penicillin/streptomycin. The cells were washed using lavage media without heparin and plated in a macrophage culture medium of RPMI-1641 supplemented with 10% FBS and penicillin/streptomycin.

HUMAN SUBJECTS AND ETHICS DECLARATION. Two patients with CAD who visited the University Hospital of Tokyo Medical and Dental University were investigated. These patients with CAD were prescribed RIV, one with and the other without, because of the complication of paroxysmal atrial fibrillation, and their samples of coronary arterial plaques were collected by debulking with directional coronary atherectomy during percutaneous coronary intervention. This research conformed to the ethical guidelines of the 1975 Declaration of Helsinki and was approved by the Ethics Committee of the Tokyo Medical and Dental University for Medical Experiments (permission number: M2000-2110); informed consent was obtained from both patients.

EVALUATION OF THE WHOLE AORTA AND SINUS PLAQUE LESIONS. Mice were sacrificed by an overdose of 3 types of mixed anesthetic agents (medetomidine, midazolam, and butorphanol at concentrations of 0.15, 2.0, and 2.5 mg/kg, respectively). The hearts and whole aortas were excised from the carcasses. The whole aortas were opened longitudinally from the ascending aorta to the iliac bifurcation, pinned en face, and stained for lipids with oil red O. The hearts were embedded in an optimal cutting temperature compound and stored at −20°C. The aortic root was serially cut into 7-μm-thick sections. A section was stained for lipids with oil red O and counterstained with hematoxylin and eosin, beginning from the point at which aortic leaflets first appeared to a position in the aorta where the valve cusps began disappearing. The stained area was identified as the atherosclerotic lesion area and evaluated as a percentage of the total aortic area using ImageJ software (National Institutes of Health).

PLASMA AND SERUM ANALYSES. At the time of sacrifice, blood was collected into heparin-coated tubes from the inferior vena cava. The blood was centrifuged at 1,500 rpm for 10 minutes at 4°C, and plasma was stored at −80°C until analysis. Prothrombin time (PT) analysis was conducted by LSI Medience. Plasma factor Xa levels were measured using commercially available kits (SensoLyte Factor Xa Assay Kit, AnaSpec). Plasma RIV concentrations were determined via liquid chromatography-mass spectrometry (Shin Nippon Biomedical Laboratories).

IMMUNOBLOT ANALYSES. RAW264.7 cells and murine primary macrophages were lysed in lysis buffer (1% Triton X-100 [Sigma-Aldrich], 50 mmol/L Tris, 150 mmol/L NaCl, and 2 mmol/L EDTA diluted with distilled water), protease inhibitor cocktail (Sigma-Aldrich), and phosphatase inhibitor cocktail tablets (PhosSTOP EASYpack, Roche Diagnostics) on ice for 10 minutes. The mixture was then centrifuged at 15,000*g* for 10 minutes, and the supernatant was analyzed via Western blotting. Equal amounts (10 μg per lane) of total proteins from each lysate were separated by sodium dodecyl sulfate-polyacrylamide gel electrophoresis and transferred to nitrocellulose membranes, which were incubated with primary antibodies overnight at 4°C, washed, and reacted with secondary antibodies for 2 hours at room temperature. Specific signals were visualized via chemiluminescence using SuperSignal West Dura Extended Duration Substrate (Thermo Scientific) and quantified using LAS-1000 image reading software (Fujifilm). Primary antibodies against the following proteins were used: LC3 (#M186-3, MBL

FIGURE 2 Continued

(A) Quantitative analysis of plasma factor Xa activity in apolipoprotein E-deficient ($ApoE^{-/-}$) mice with or without a high-fat diet (HFD) and rivaroxaban (RIV) 120 mg/kg/d. *$P < 0.05$ (n = 7). **(B) (Top)** Representative images of the aorta en face stained with oil red O. **(Bottom)** Quantitative analysis of the area of atherosclerotic plaques in the aorta. *$P < 0.05$ (n = 10). **(C) (Top)** Representative pictures of Mallory-Azan–stained aortic root plaques. **(Bottom)** Quantitative analysis of the area of aortic root plaques. *$P < 0.05$ (n = 10). All data are expressed as **dot plots**, with **lines** indicating the mean ± standard error of the mean.

FIGURE 3 **The Effects of Factor Xa on Macrophage Autophagy Both In Vivo and In Vitro**

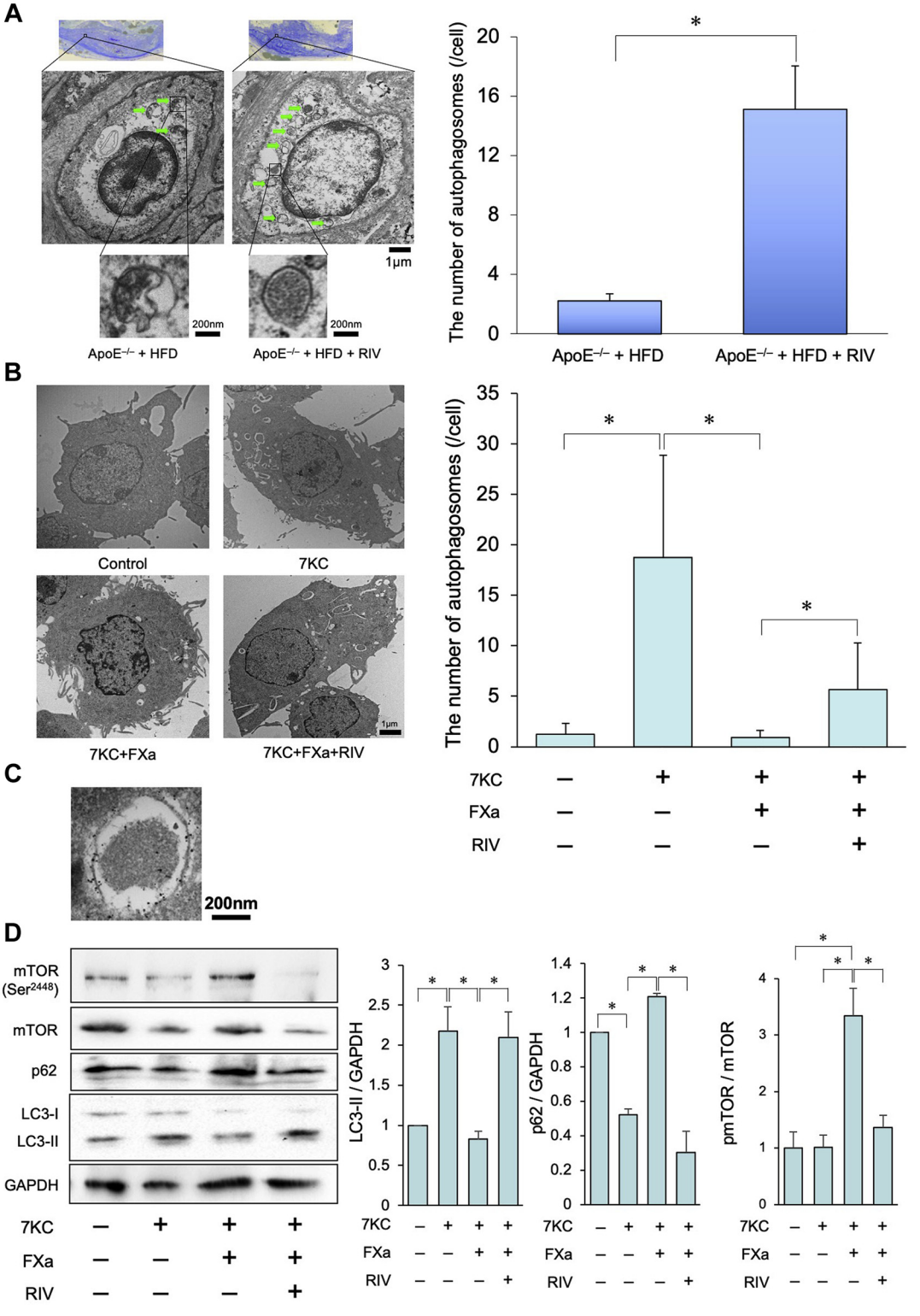

Continued on the next page

International), p62 (#PM045, MBL International), mTOR (#2983, Cell Signaling Technologies), phospho-mTOR (Ser2448) (#5536, Cell Signaling Technologies), NLR family pyrin domain containing 3 (NLRP3) (#A017374, Atlas Antibodies), caspase-1 (#ab108362, Abcam), ASC (#D086-3, MBL International), TRIM20 (Pyrin) (#ab195975, Abcam,), GAPDH (#2118, Cell Signaling Technologies), cleaved interleukin (IL)-1β (Asp117) (#63124, Cell Signaling Technologies), ULK1 (#8054, Cell Signaling Technologies), phospho-ULK1 (Ser317) (#37762, Cell Signaling Technologies), phospho-ULK1 (Ser757) (#14202, Cell Signaling Technologies), Beclin1 (#3738, Cell Signaling Technologies), ATG16L1 (#8089, Cell Signaling Technologies), and β-actin (#4970, Cell Signaling Technologies).

ENZYME-LINKED IMMUNOSORBENT ASSAY. The culture media of RAW264.7 cells or murine primary macrophages was analyzed via enzyme-linked immunosorbent assay (ELISA) for the levels of IL-1β (Human IL-1β ELISA MAX Deluxe Set, BioLegend) according to the manufacturer's protocols.

IN SITU PROXIMITY LIGATION ASSAY AND IMMUNOFLUORESCENCE. RAW264.7 cells seeded on chamber slides were fixed on cold methanol for 10 minutes. After washing with phosphate-buffered saline (PBS) and permeabilization with 1% Triton X-100, the cells were processed for immunofluorescence proximity ligation assay (PLA). For immunofluorescence, RAW264.7 cells were incubated with blocking buffer (5% bovine serum albumin [BSA] and 0.1% Triton X-100) and then with the primary antibodies overnight at 4°C. After washing with PBS, Alexa Fluor–conjugated (488) (ThermoFisher Scientific) secondary antibody was applied with the blocking buffer. Finally, coverslips were mounted on the slides using VECTASHIELD with DAPI (Vector Labs) and photographed. PLA was performed on the chamber slides according to the Duolink in situ solutions manual (Sigma-Aldrich). We generated PLA probes conjugating primary antibodies with a PLUS or MINUS oligonucleotide. We followed using the Duolink In Situ Probemaker PLUS for the TRIM20 antibody (Cell Signaling Technologies) and MINUS for the NLRP3 antibody (NB100-122, Cell Signaling Technologies). After blocking, RAW264.7 cells were incubated with combinations of NLRP3 probe (−) and TRIM20 probe (+) overnight at 4°C in a humidified chamber. After washing, the ligation and amplification steps were performed as described using the Duolink In Situ Detection Reagent Green (Cell Signaling Technologies). After the final washes, the specimens were mounted on the chamber slides using VECTASHIELD with DAPI.

TRANSMISSION ELECTRON MICROSCOPY. Cultured cells were fixed in 2.5% glutaraldehyde in 0.1 mol/L phosphate buffer (PB) for 2 hours, washed with 0.1 mol/L PB, postfixed in 1% osmium tetroxide in 0.1 mol/L PB for 2 hours, dehydrated in a graded series of ethanol, and embedded in Epon 812 (TAAB Laboratory Equipment). Semithin sections were cut at a thickness of 1 μm and stained with toluidine blue. Ultrathin 90-nm sections were collected on copper grids, double stained with uranyl acetate and lead citrate, and then observed under a transmission electron microscope (H7011, Hitachi High-tech). Autophagosomes in transmission electron microscopy were determined under the supervision of an expert at the Tissue Analyzing Unit in Research Core Center of Tokyo Medical and Dental University (24).

IMMUNOELECTRON MICROSCOPY. Cultured cells were blocked in PBS with 5% BSA at room temperature for 30 minutes. The samples were incubated with a primary antibody against LC3 diluted 1:200 in 5% BSA at 4°C overnight. After rinsing in 0.1 mol/L PB containing 0.005% saponin, the samples were incubated with a second antibody (Qdot 655 goat F[ab']2 antirabbit IgG conjugate (H + L) [1:200], Invitrogen) at room temperature for 2 hours. The samples were washed with 0.005% saponin in 0.1 mol/L PB and then with 0.1 mol/L PB and fixed in 1% glutaraldehyde in 0.1 mol/L PB for 10 minutes. After washing with 0.1 mol/L PB and distilled water, the samples were fixed

FIGURE 3 Continued

(A) (Left) Representative transmission electron microscopic images of autophagosomes (**arrows and insets**) in macrophages derived from the atheroma of high-fat diet (HFD)-fed apolipoprotein E–deficient ($ApoE^{-/-}$) mice with or without rivaroxaban (RIV) administration. **(Right)** Quantitative analysis of the number of autophagosomes in macrophages residing in the atheroma with or without RIV. $^*P < 0.05$ (n = 10). **(B) (Left)** Representative transmission electron microscopic images of autophagosomes in RAW264.7 macrophages with and without the administration of indicated compounds. **(Right)** Quantitative analysis of the number of autophagosomes with and without the administration of indicated compounds. $^*P < 0.05$ (n = 10). **(C)** A representative immunoelectron microscopic image of autophagosomes stained with anti-LC3 antibody in 7KC-treated RAW264.7 macrophages. **(D) (Left)** Representative immunoblot images of mammalian target of rapamycin (mTOR), phospho-mTOR (pmTOR) (Ser^{2448}), p62, LC3, and glyceraldehyde 3-phosphate dehydrogenase (GAPDH). **(Right)** Densitometric analysis of immunoblots. $^*P < 0.05$ (n = 3). All data are expressed as mean ± standard error of the mean.

FIGURE 4 **The Effects of Factor Xa on NLRP3 Inflammasomes of Macrophages Both In Vivo and In Vitro**

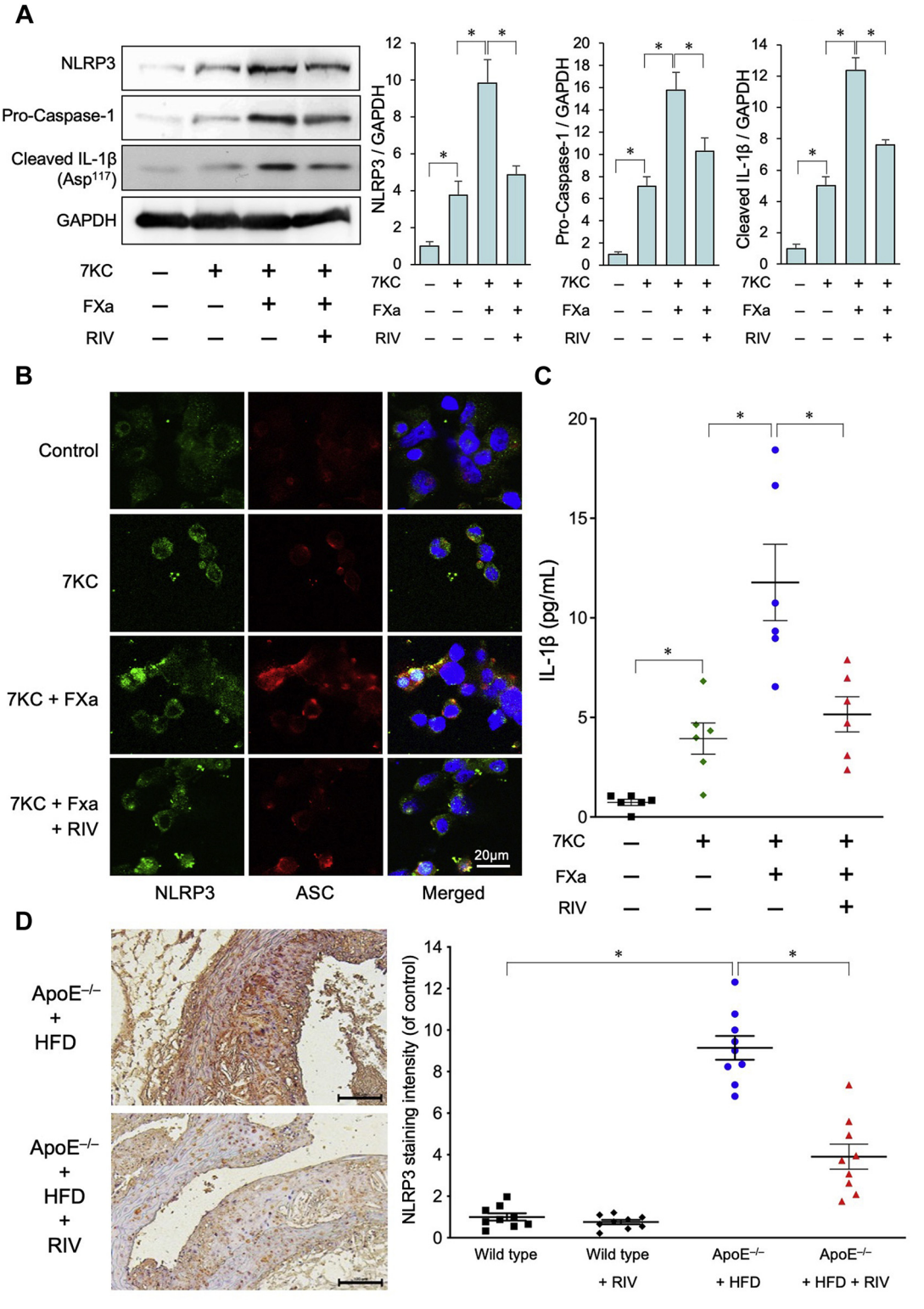

Continued on the next page

in 0.3% osmium tetroxide in 0.1 mol/L PB for 17 minutes. Subsequently, the samples were washed with 0.1 mol/L PB, dehydrated in ethanol, and stained with 2% uranyl acetate in 70% ethanol at 4°C for 1 hour. The samples were dehydrated in a graded series of ethanol and embedded in Epon 812 for 48 hours. Ultrathin 70-nm to 80-nm-thick sections were collected on copper grids and then observed under a transmission electron microscope.

STATISTICS. All statistical analyses were conducted using the IBM SPSS Statistics 22 software (SPSS Japan Institute). The normality of distribution was determined using a D'Agostino-Pearson normality test and confirmed that all data were normally distributed. All statistical data are expressed as mean ± SEM. All statistical analyses were performed using an unpaired Student's *t*-test or 1-way analysis of variance followed by post hoc Bonferroni-Dunn method for multiple pairwise comparisons. In all cases, the results were considered statistically significant at a *P* value <0.05.

RESULTS

PHARMACOLOGIC EFFECTS OF RIV IN MICE. To evaluate RIV's pharmacologic effects in mice, we measured the RIV plasma concentration, plasma factor Xa activity, and PT. Mice were randomized to controls and those treated with polyethylene glycol 400-aggregated RIV (60 or 120 mg/kg/d) for 1 week. Treatment with RIV significantly increased the plasma RIV concentration and effectively suppressed plasma factor Xa activity in a dose-dependent manner (**Figures 1A and 1B**). The administration of 120 mg/kg/d RIV to the mice significantly suppressed plasma factor Xa activity by 55% and effectively elongated PT, similar to patients taking clinical doses of RIV (**Figures 1B and 1C**). However, with regard to the value of activated partial thromboplastin time of the plasma, no significant difference was observed among the 3 groups (**Figure 1D**). These results suggest that the administration of 120 mg/kg/d RIV effectively suppressed factor Xa activity, thereby attenuating blood clotting ability in mice.

THE EFFECT OF RIV ON ATHEROSCLEROTIC PLAQUES IN HFD-FED ApoE$^{-/-}$ mice. Plasma factor Xa activity in HFD-fed ApoE$^{-/-}$ mice was remarkably higher than in WT mice, and RIV administration significantly suppressed plasma factor Xa activity in HFD-fed ApoE$^{-/-}$ mice (**Figure 2A**). We evaluated the effect of RIV on aortic atherosclerotic plaques. In HFD-fed ApoE$^{-/-}$ mice, RIV administration significantly attenuated the atherosclerotic areas in the whole aorta (**Figure 2B**) and the aortic sinus (**Figure 2C**). These results indicate that RIV administration could effectively suppress atherosclerotic plaques in HFD-fed ApoE$^{-/-}$ mice.

FACTOR XA INHIBITS MACROPHAGE AUTOPHAGY THROUGH mTOR ACTIVATION. Ultrastructural examinations of atherosclerotic lesions of HFD-fed ApoE$^{-/-}$ mice were conducted via transmission electron microscopy. A greater number of autophagosomes (green arrows in **Figure 3A**) were observed in macrophages residing in the atheroma of RIV-treated mice than in the untreated mice, suggesting that the autophagy activity of macrophages in atheroma is enhanced by treatment with RIV (**Figure 3A**). A similar tendency was observed in macrophages residing in the atheroma of coronary arterial plaques debulked with directional coronary atherectomy in patients with CAD who were prescribed RIV compared with those patients without RIV (Supplemental Figure 1).

To test whether factor Xa and RIV affect macrophage autophagy in vitro, the effect of 7KC, an atherosclerotic lesional oxysterol that promotes oxidative stress and inflammation, on autophagy activity was evaluated in RAW264.7 macrophages. Transmission electron microscopic analyses demonstrated that treatment with 7KC significantly increased the number of autophagosomes (**Figure 3B**), which was confirmed by immunoelectron microscopic examinations in RAW264.7 cells (**Figure 3C**). Immunoblot analyses indicated that treatment with 7KC

FIGURE 4 Continued

(A) (Left) Representative immunoblot images of NLR family pyrin domain containing 3 (NLRP3), caspase-1, interleukin (IL)-1β, and GAPDH. **(Right)** Densitometric analysis of immunoblots. **P* < 0.05 (n = 3). All data are expressed as mean ± standard error of the mean. **(B)** Immunohistochemical images of NLRP3 inflammasome markers in RAW264.7 macrophages with and without the administration of indicated compounds. **(C)** RAW264.7 macrophages with and without the administration of indicated compounds were analyzed for IL-1β secretion in the supernatants by enzyme-linked immunosorbent assay. **P* < 0.05 (n = 6). Data are expressed as **dot plots**, with the **lines** indicating the mean ± standard error of the mean. **(D) (Left)** Representative images of NLRP3 immunostaining in atheromas derived from high-fat diet–fed apolipoprotein E knockout (KO) mice with or without the rivaroxaban administration. **(Right)** Quantitative analysis of the number of NLRP3 staining intensity in immunohistochemical samples. **P* < 0.05 (n = 9). Data are expressed as **dot plots**, with the **lines** indicating the mean ± standard error of the mean. WT = wild type.

FIGURE 5 **The Role of Protease-Activated Receptor 2–Mediated Signaling in Regulating Autophagy and NLRP3 Inflammasome Both on PAR2 Knockout and WT Mice-Derived Macrophages**

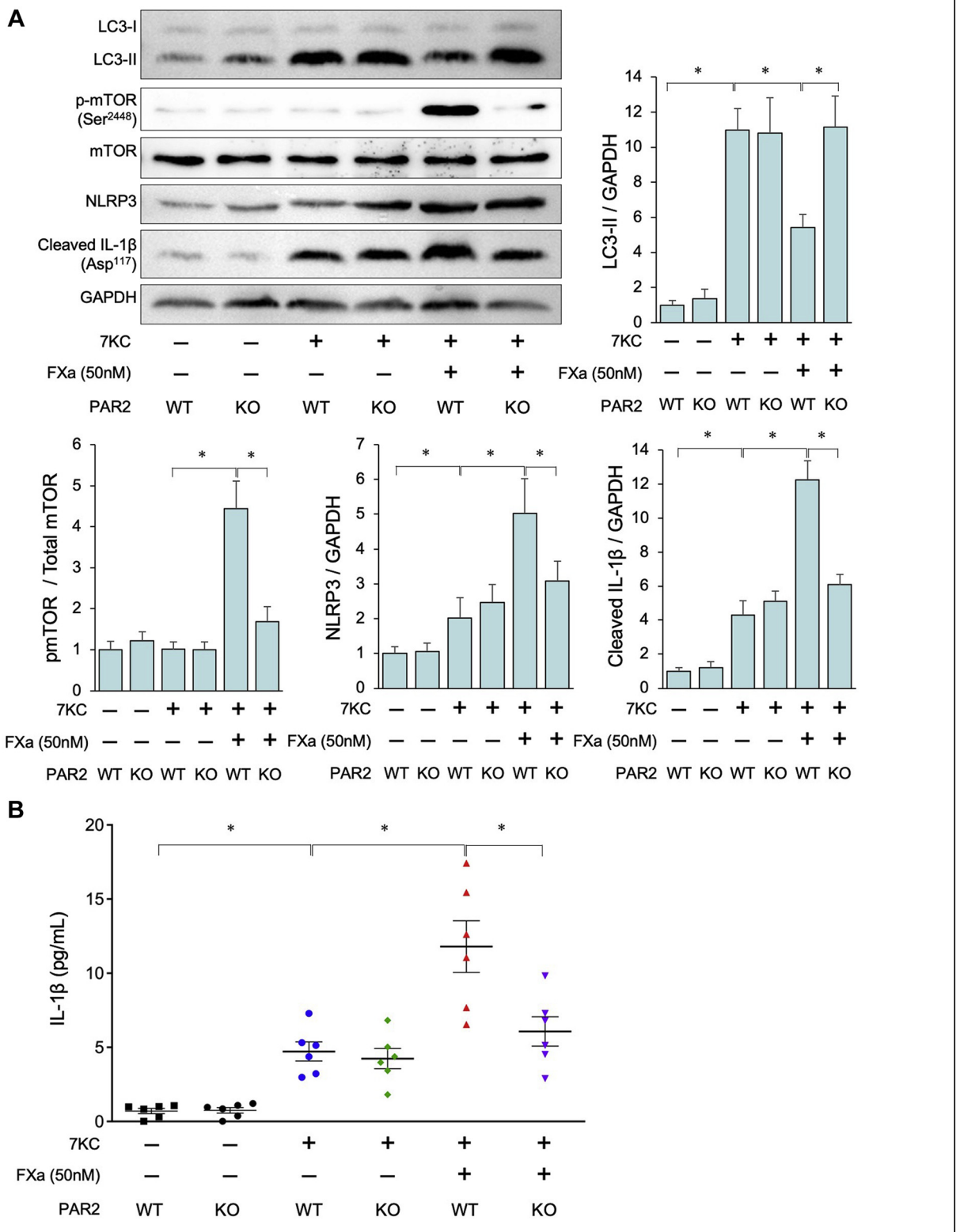

Continued on the next page

significantly enhanced the accumulation of LC3-II protein in RAW264.7 cells (Figure 3D), suggesting that 7KC significantly promotes autophagy in RAW264.7 cells. Treatment with factor Xa significantly suppressed 7KC-induced autophagy, and this inhibitory effect was reversed by the addition of RIV, as evidenced by the number of autophagosomes observed via transmission electron microscopy (Figure 3B). Immunoblot analyses consistently indicated that factor Xa significantly reduced the amount of LC3-II that was up-regulated by 7KC, and this inhibitory effect was reversed by the addition of RIV (Figure 3D). The increase in mTOR phosphorylation induced by the treatment of factor Xa was canceled in the presence of RIV (Figure 3D). These results suggest that factor Xa inhibits 7KC-induced autophagy through the activation of mTOR, which was reversed in the presence of RIV.

FACTOR XA ENHANCES INFLAMMASOME FORMATION BOTH IN THE 7KC-TREATED MACROPHAGES AND MURINE ATHEROMAS. There is a growing body of evidence that suggests the activation of inflammasome, an innate immune complex, is closely associated with atherogenesis (25). It has also been shown that the antiatherosclerotic effect of autophagy is mediated through inflammasome suppression (22). Based on these backgrounds, the next test determined whether factor Xa is involved in inflammasome activation. Treatment with 7KC led to a substantial increase in inflammasome activation in macrophages. This is evidenced by the accumulation of NLRP3, pro-caspase-1, and pro-IL-1β proteins (by immunoblotting, Figure 4A); an increased amount of NLRP3 colocalized with ASC in RAW264.7 cells (by immunofluorescence analyses, Figure 4B); and elevation of the IL-1β level in the culture media of RAW264.7 cells (by ELISA, Figure 4C). Treatment with factor Xa significantly enhanced 7KC-induced inflammasome formation. This effect was attenuated by the addition of RIV, as evidenced by the immunoblot and immunofluorescence analyses and ELISA (Figures 4A and 4C). Immunostaining of atheromas derived from HFD-fed ApoE$^{-/-}$ mice was performed, and there was a significant increase in NLRP3-positive cells accumulated in the atheromas of untreated mice. Conversely, the accumulation of NLRP3-positive cells in the atheromas was significantly suppressed by RIV treatment (Figure 4D). These results indicate that RIV treatment could effectively reduce inflammasome formation in the factor Xa-treated macrophages and atherosclerotic lesions.

FACTOR XA PROMOTES INFLAMMASOME ACTIVITY THROUGH PAR2-MEDIATED SUPPRESSION OF AUTOPHAGY 7KC-TREATED MACROPHAGES. We examined whether factor Xa-induced autophagy inhibition and subsequent inflammasome activation are mediated through PAR2. Macrophages taken from both PAR2$^{-/-}$ and WT mice were treated with 7KC, with and without factor Xa. Treatment with factor Xa significantly suppressed autophagy and markedly enhanced the formation of inflammasomes in WT macrophages (Figures 5A and 5B). However, treatment with factor Xa did not affect either the autophagy or inflammasome activity in PAR2-deficient macrophages (Figures 5A and 5B). The level of phosphorylated mTOR was not elevated in PAR2-deficient macrophages, even in the presence of factor Xa (Figure 5A). These results indicate that factor Xa promotes inflammasome activity, possibly through the PAR2-mediated suppression of autophagy.

INFLAMMASOMES ARE DEGRADED BY TRIM20-MEDIATED PRECISION AUTOPHAGY IN 7KC-TREATED MACROPHAGES. Previous investigations have demonstrated that the key components of inflammasomes, including NLRP3, are degraded by highly specific autophagy (precision autophagy) (26). Based on these previous findings, we evaluated whether NLRP3 could be degraded by precision autophagy. TRIM20, a specialized receptor of precision autophagy, interacts with ULK1, Beclin1, and ATG16L1 to initiate precision autophagy. Through immunoprecipitation assays, we found that treatment with 7KC promoted protein-protein interactions between TRIM20 and ULK1, in addition to Beclin1 and ATG16L1, in RAW264.7 cells (Figure 6A). It was also determined that treatment with 7KC promoted protein-protein interaction between NLRP3 and TRIM20 (Figure 6B). We next evaluated the effect of

FIGURE 5 Continued

(A) (Top) Representative immunoblot images of LC3, phospho–mammalian target of rapamycin (p-mTOR), mammalian target of rapamycin (mTOR), NLR family pyrin domain containing 3 (NLRP3), interleukin (IL)-1β, and glyceraldehyde 3-phosphate dehydrogenase (GAPDH). **(Bottom)** Densitometric analysis of immunoblots. *$P <$ 0.05 (n = 3). All data are expressed as mean ± standard error of the mean. **(B)** Macrophages taken from both protease-activated receptor 2 **(**PAR2) knockout (KO) and wild-type (WT) mice with and without the administration of indicated compounds were analyzed for IL-1β secretion in the supernatants by enzyme-linked immunosorbent assay. *$P < 0.05$ (n = 6). Data are expressed as **dot plots**, with the lines indicating the mean ± standard error of the mean.

FIGURE 6 The Inflammasome Is Degraded by TRIM20-Mediated Precision Autophagy in 7-Ketocholesterol-Treated RAW264.7 Macrophages

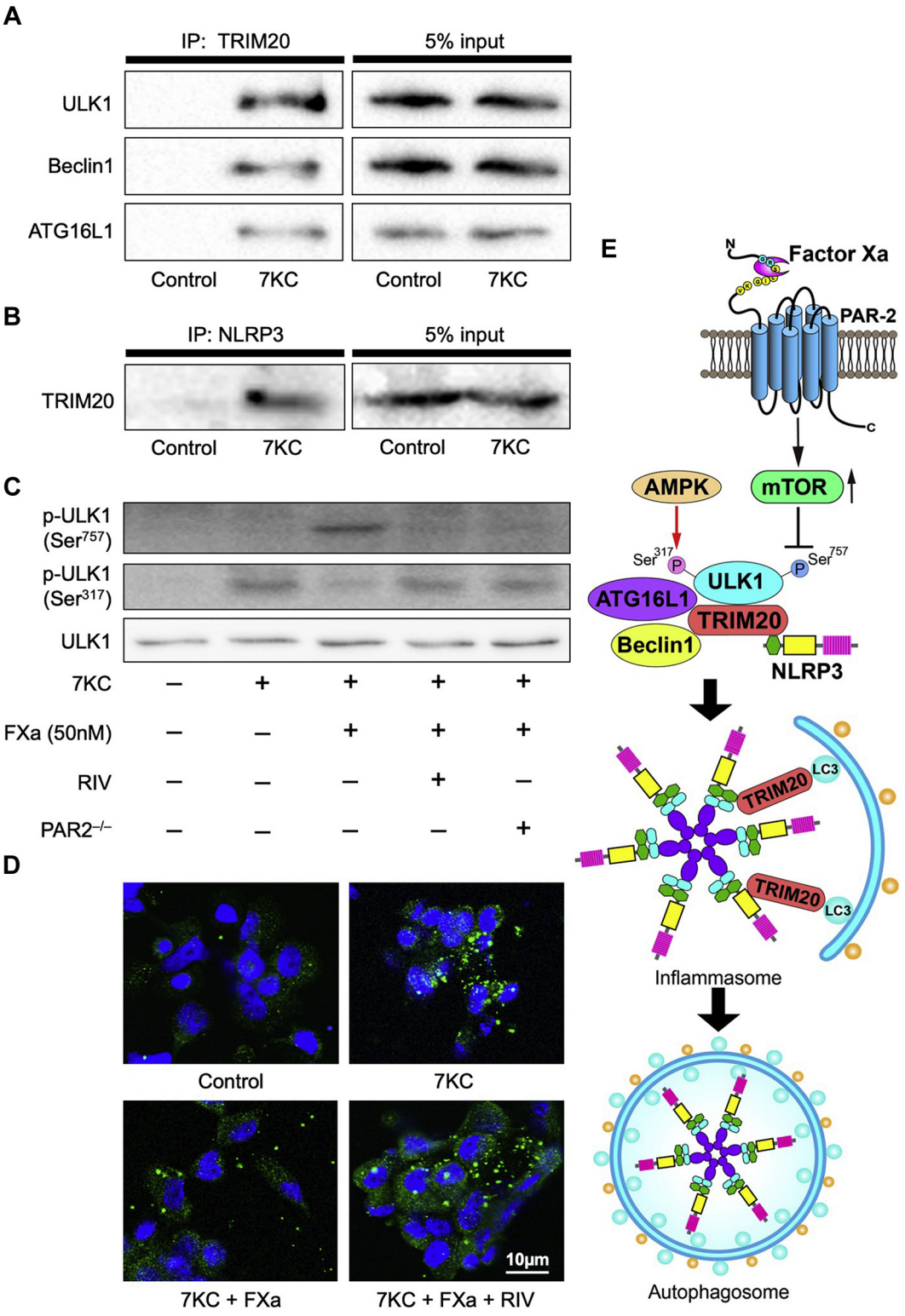

Continued on the next page

factor Xa-PAR2 signaling on precision autophagy. Cotreatment with 7KC and factor Xa significantly increased the level of phosphorylated ULK1-Ser757, an inactive form of ULK1 phosphorylated by mTOR, in WT macrophages (Figure 6C). However, treatment with factor Xa did not affect the level of phosphorylated ULK1-Ser757 in PAR2-deficient macrophages (Figure 6C). Treatment with 7KC led to a substantial increase in the level of phosphorylated ULK1-Ser317, an active form of ULK1 phosphorylated by adenosine triphosphate-activated protein kinase, both in WT and PAR2-deficient macrophages (Figure 6C). Treatment with factor Xa significantly reduced the level of phosphorylated ULK1-Ser317 in WT macrophages, which was reversed by the addition of RIV (Figure 6C). Consistently, in situ PLA assays demonstrated that the 7KC-induced interaction between NLRP3 and TRIM20 in RAW264.7 cells was reduced by the presence of factor Xa, which was reversed by the administration of RIV (Figure 6D). These results suggest that NLRP3, a major component of the NLRP3 inflammasome, is degraded by TRIM20-mediated precision autophagy in a factor Xa-PAR2-dependent manner in 7KC-treated macrophages.

PAR2-MEDIATED ATHEROGENESIS IS PARTIALLY MEDIATED THROUGH AUTOPHAGY SUPPRESSION. To further study the in vivo relevance of atherosclerosis by factor Xa-PAR2-mediated autophagy inhibition, RIV or chloroquine (CQ) (an inhibitor of autophagy flux) was administered to the set of mice and the examined plaque area (Figure 7A). The administration of CQ significantly inhibited autophagy flux in atheromatous plaques in mice, as evidenced by the immunoblot analyses of both LC3-II and p62 (Supplemental Figure 2). The atherosclerotic areas in the whole aorta were markedly smaller in HFD-fed ApoE$^{-/-}$/PAR2$^{-/-}$ bigenic mice than in HFD-fed ApoE$^{-/-}$ mice (Figure 7B). The atherosclerotic lesions of the whole aorta in ApoE$^{-/-}$/PAR2$^{-/-}$ bigenic mice treated with RIV were significantly reduced compared with those of untreated mice (Figure 7B). We also found that the administration of CQ to HFD-fed ApoE$^{-/-}$/PAR2$^{-/-}$ bigenic mice significantly increased the appearance of atherosclerotic areas, both in the whole aorta and the sinus, compared with untreated mice (Figure 7B). Similar effects to those described earlier were observed in the aortic sinus atherosclerotic areas of each mouse group (Supplemental Figure 3).

These results indicate that PAR2 mediates the progression of atherosclerosis by inhibiting autophagy and that RIV might prevent plaque progression through the inhibition of PAR2 signaling and other pathways.

DISCUSSION

It was demonstrated that RIV effectively suppresses atherogenesis via a PAR2-mediated pathway through the activation of autophagy, in turn inhibiting inflammasome formation in macrophages. The major findings of this study are as follows: 1) the administration of an optimal dosage of RIV to mice effectively attenuates atherosclerosis; 2) factor Xa enhances mTOR phosphorylation, thereby suppressing 7KC-induced macrophage autophagy; 3) factor Xa promotes inflammasome activation; 4) PAR2-mediated signaling aggravates atherosclerotic plaque progression by inhibiting autophagy; and 5) the suppression of autophagy abrogates the salutary effect of RIV on atherogenesis.

There are findings from previous studies supporting the antiatherosclerotic effects of RIV (12); however, other studies do not support this effect (27). In studies that do not support the protective effect of RIV against atherosclerosis, factor Xa activities were not sufficiently suppressed, possibly as a result of the small dosage of RIV (5 mg/kg/d). The prolongation of PT was not observed when 5 mg/kg/d RIV was administered to mice. To solve this problem, the optimal dosage of RIV to effectively suppress factor Xa activities in mice was determined. A previous clinical pharmacodynamic and pharmacokinetic study demonstrated that the administration of RIV for humans at total daily oral doses of 5 to 80 mg resulted in a maximum drug concentration of RIV ranging from 119 to 316 μg/L (mean values) and median inhibitions of factor Xa activities ranging from 20% to 61% (28). On the other hand, the data

FIGURE 6 Continued

(A) Lysates from RAW264.7 macrophages treated with or without 7-ketocholesterol (7KC) were subjected to immunoprecipitation with the anti-TRIM20 antibody. The immunoprecipitants and 5% inputs were immunoblotted with the anti-ULK1, anti-Beclin1, and anti-ATG16L1 antibodies. **(B)** Lysates from RAW264.7 macrophages treated with or without 7KC were subjected to immunoprecipitation with the anti-NLR family pyrin domain containing 3 (NLRP3) antibody. The immunoprecipitants and 5% inputs were immunoblotted with the anti-TRIM20 antibody. **(C)** Representative immunoblot images of p-ULK1(Ser^{317}), p-ULK1(Ser^{757}), and total ULK1. **(D)** The representative images of in situ proximity ligation assays. **Green dots** indicate the NLRP3-TRIM20 interaction in RAW264.7 macrophages. **(E)** A schematic representation of precision autophagy. NLRP3 inflammasome is degraded by precision autophagy through the TRIM20-mediated mechanism. IP = immunoprecipitation.

FIGURE 7 The Role of Both PAR2 and Autophagy in the Progression of Atherosclerosis in a HFD-fed Apo$^{-/-}$ Knockout Mice

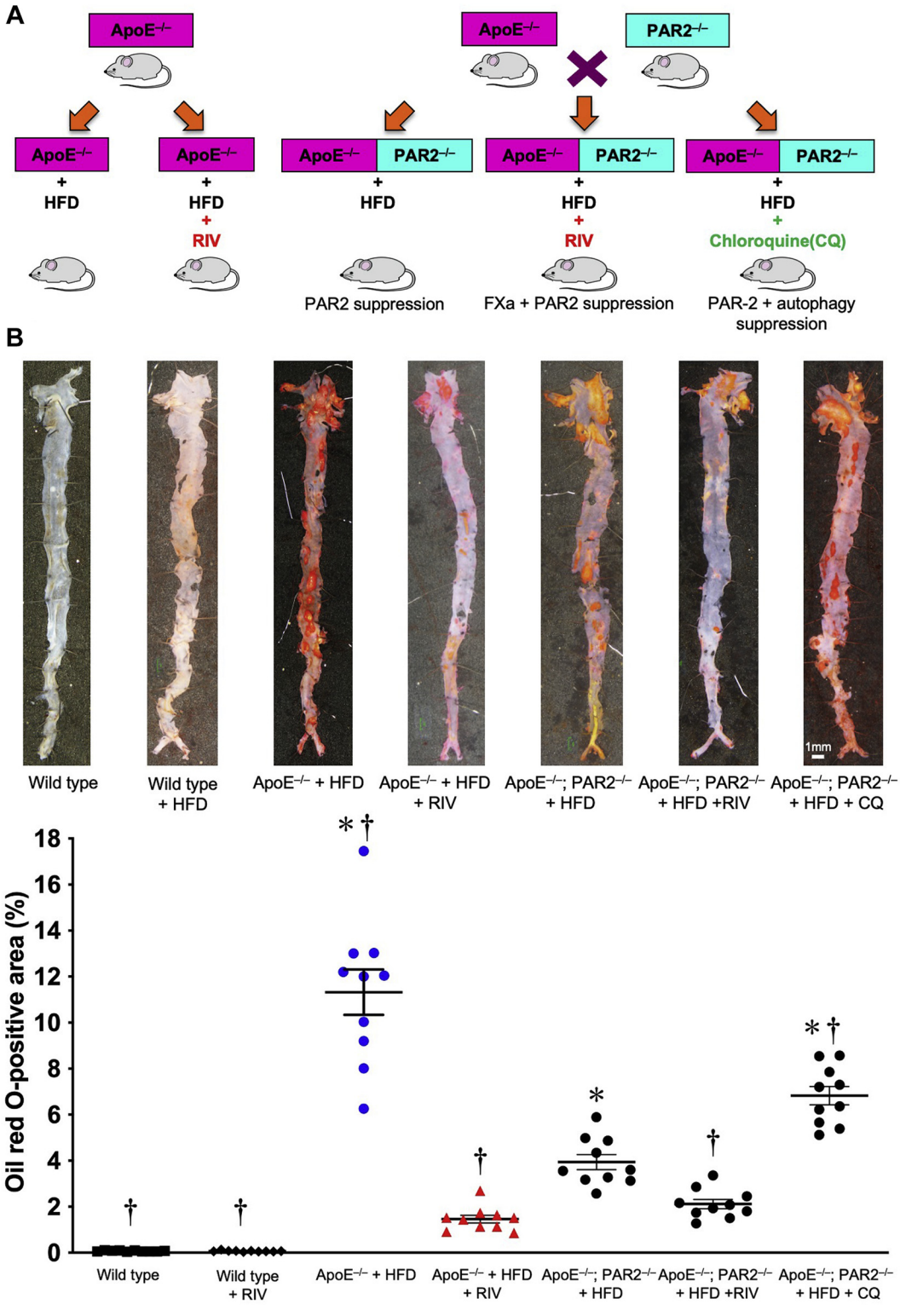

Continued on the next page

presented here suggest that the plasma RIV concentration in the mice after 120 mg/kg/d RIV administration was 824.2 μg/L (mean values), 2.6- to 6.9-fold higher than that of humans who were administered RIV within clinically relevant doses. Although such an amount of RIV dosage is excessive for humans, it is acceptable for mice because of the differences in metabolic systems between humans and mice. The dosage of 120 mg/kg/d RIV administration significantly suppressed plasma factor Xa activity by 55% in mice. None of the mice treated with 120 mg/kg/d RIV suffered any fatal hemorrhagic complication. It was determined that 120 mg/kg/d is an appropriate dosage of RIV to suppress plasma factor Xa activity to mimic clinical usage in mice.

There is another fundamental question regarding how RIV affects macrophages inside the arterial wall. Previous studies have shown that factor Xa is present in atherosclerotic plaques and in the plasma (29), possibly as a result of excretion from macrophages (30). Because RIV is a lipophilic compound, it is possible that RIV affects atheroma-resident macrophages by permeating through arterial walls, thereby inhibiting atherosclerotic plaque-localizing factor Xa activity. To ascertain this hypothesis, further investigations need to be conducted in the future.

Increasing lines of evidence suggest that PAR2 plays a significant role in the progression of vascular inflammation, which aggravates atherosclerosis (20). A previous report indicated that PAR2 negatively regulates autophagy via mTOR signaling (31). With the previous findings that autophagy suppression promotes atherosclerosis by enhancing vascular inflammation (21,22), it was hypothesized that factor Xa–mediated PAR2 activation might play a critical role in the progression of atherosclerosis, partially through the down-regulation of autophagy machinery. As expected, the administration of factor Xa enhanced mTOR phosphorylation and 7KC-induced autophagy activity, which were inhibited by the ablation of the PAR2 gene in cultured macrophages. We also observed that the atherosclerotic plaque areas of CQ-treated ApoE$^{-/-}$/PAR2$^{-/-}$ bigenic mice were significantly increased compared with those of untreated mice. These results indicate that autophagy machinery might play a crucial role in the formation of arteriosclerosis through PAR2-mediated signaling.

One of the major roles of autophagy is to eliminate danger signals in the cells, including damaged mitochondria and excessively activated inflammasome, a molecular complex suppressing the inflammatory response caused by natural immunity. Yan et al (32) demonstrated that the NLRP3 inflammasome is negatively regulated by cyclic adenosine monophosphate–dependent molecule-specific selective autophagy through the activation of MARCH7, an E3 ubiquitin-protein ligase. Kimura et al (26) reported that TRIM20 acts as a specialized receptor for precision autophagy of key components of the inflammasome and type I interferon response systems. It was demonstrated here that NLRP3 is degraded by TRIM20-mediated precision autophagy in 7KC-treated macrophages. Taken in conjunction with the fact that the inflammasome exacerbates atherosclerosis by promoting sterile inflammation triggered by damage-associated molecular patterns (25), it makes sense that inflammasome activity dysregulation promotes atherosclerosis, in part through the suppression of autophagy machinery, as reported by Razani et al (22). This study also demonstrated that factor Xa facilitates IL-1ß release by NLRP3 inflammasome activation, which was reversed by the administration of RIV. A growing body of clinical evidence suggests that anti-inflammasome agents, such as canakinumab and colchicine, could effectively reduce recurrent cardiovascular events (33,34). This evidence leads us to believe that the PAR2 signal activated by factor Xa inhibits the degradation of the NLRP3 inflammasome by suppressing autophagy and facilitating the inflammation of blood vessels related to the formation of arteriosclerosis.

Our study demonstrated that the area of atherosclerotic plaque significantly decreased in RIV-treated ApoE$^{-/-}$/PAR2$^{-/-}$ bigenic mice compared with that of untreated mice. This result shows that there

FIGURE 7 Continued

(A) A schematic of the experimental design for evaluating the effect of factor Xa–PAR2-mediated autophagy regulation on atherosclerosis. ApoE$^{-/-}$ mice, ApoE$^{-/-}$/protease-activated receptor 2 (PAR2) knockout (PAR2$^{-/-}$) bigenic mice, or wild-type mice were fed a high-fat diet (HFD) for 20 weeks with or without treatment with rivaroxaban (RIV) or chloroquine (CQ) (an autophagy inhibitor). The mice were sacrificed for analyses after 20 weeks. **(B) (Top)** Representative images of the aorta en face derived from HFD-fed ApoE$^{-/-}$ mice, ApoE$^{-/-}$/PAR2$^{-/-}$ bigenic mice, or wild-type mice with and without the administration of RIV and CQ stained with oil red O. **(Bottom)** Quantification of aortic en face plaque area in HFD-fed ApoE$^{-/-}$ mice or ApoE$^{-/-}$/PAR2$^{-/-}$ bigenic mice, as shown in the representative images. *$P < 0.05$ versus ApoE$^{-/-}$ + HFD + Riv(+). †$P < 0.05$ versus ApoE$^{-/-}$;PAR2$^{-/-}$ + HFD (n = 10). Data are expressed as **dot plots**, with **line**s indicating the mean ± standard error of the mean. ApoE$^{-/-}$ = apolipoprotein E; HFD = high-fat diet; PAR2 = protease-activated receptor-2.

are pathways other than the PAR2 pathway in which factor Xa facilitates arteriosclerosis. Recently, Petzold et al (35) suggested that RIV inhibits the factor Xa-mediated activation of protease-activated receptor 1, thereby suppressing platelet activity (35). Taken in conjunction with the fact that platelets play a significant role in the process of atherogenesis (36), the protherosclerotic activity of factor Xa would be mediated through the dual suppression of protease-activated receptor 1- and PAR2-mediated signaling. Such a mechanism could explain how RIV monotherapy may prevent cardiovascular events, comparable with combination therapy with RIV plus a single antiplatelet agent, in patients with atrial fibrillation and stable CAD. This was previously demonstrated by the AFIRE (Atrial Fibrillation and Ischemic Events With Rivaroxaban in Patients With Stable Coronary Artery Disease) trial (37). In this regard, further studies are needed.

STUDY LIMITATIONS. There should be the consideration that there is a potential limitation to the strategy of autophagy inhibition in our experiments as CQ is not a specific autophagy inhibitor. To ascertain these findings, additional *in vivo* experiments using a more specific loss-of-function model of autophagy, such as macrophage-specific Atg5 knockout mice, should be conducted in the future.

There is another limitation in this study regarding the experiments using human samples. We evaluated the effect of RIV on macrophages residing in human atherosclerotic plaques and observed that the number of autophagosomes in macrophages residing in the atheroma of coronary arterial plaques with RIV tended to be greater than that without RIV However, as the number of samples in each group was n = 1, a further investigation with a greater number of samples should be conducted to increase the reliability of this result in the future.

CONCLUSIONS

Our current study revealed that factor Xa-PAR2 signaling promotes atherogenesis by accelerating inflammasome activities through the suppression of autophagy. This suggests that RIV could be a useful antiatherosclerotic agent.

ACKNOWLEDGMENTS The authors thank Ms Noriko Tamura (pathological experiments; Department of Cardiovascular Medicine, Tokyo Medical and Dental University), Ms Yuriko Sakamaki (electron microscopic experiments; Tissue Analyzing Unit in Research Core Center of Tokyo Medical and Dental University), and Dr Takashi Ashikaga (percutaneous coronary intervention including directional coronary atherectomy; Department of Cardiovascular Medicine, Tokyo Medical and Dental University/ Musashino Red-Cross Hospital) for their excellent technical assistance. We also thank Bayer AG for providing RIV.

FUNDING SUPPORT AND AUTHOR DISCLOSURES

This work was supported in part by a grant from Bayer Yakuhin Ltd and JSPS KAKENHI Grant-in-Aid for Scientific Research (C) (17K09570 to Dr Maejima). Dr Maejima has received speaker honoraria from Bayer, Boehringer Ingelheim, and AstraZeneca; and research support from AstraZeneca, Boehringer Ingelheim, Bayer, Bristol-Myers Squibb, Chugai Pharmaceuticals, Eli Lilly, MSD, and Novartis Pharma. All other authors have reported that they have no relationships relevant to the contents of this paper to disclose.

ADDRESS FOR CORRESPONDENCE: Dr Yasuhiro Maejima, Department of Cardiovascular Medicine, Tokyo Medical and Dental University, 1-5-45 Yushima, Bunkyo-ku, Tokyo 113-8519, Japan. E-mail: ymaeji.cvm@tmd.ac.jp.

PERSPECTIVES

COMPETENCY IN MEDICAL KNOWLEDGE: Despite the large number of drug therapies for the treatment of atherosclerosis, there is still a compelling need for establishing a novel and effective therapy because the efficacy of existing therapies for the prevention of atherosclerotic lesions is only 30% to 40%. We evaluated the impact of RIV, a direct oral factor Xa inhibitor, on experimental atherosclerotic models and explored the molecular mechanisms underlying the aggravation of atherosclerosis induced by factor Xa.

TRANSLATIONAL OUTLOOK: Several large-scale clinical trials, including the ATLAS ACS 2-TIMI 51 study and the COMPASS trial, have demonstrated that RIV administration could reduce the risk of death from CADs. Based on such landmark achievements, the U.S. Food and Drug Administration has approved RIV for reducing the risk of major cardiovascular events in people with chronic coronary or peripheral artery diseases. However, it is important to determine the mechanism by which RIV suppresses atherosclerosis to establish RIV as a novel antiatherosclerotic drug worldwide. Current findings demonstrate that RIV alleviates atherosclerosis by blocking the factor Xa–PAR2-mediated inhibition of macrophage autophagy, in turn attenuating inflammasome activity, and may provide strong mechanistic evidence for the clinical use of RIV.

REFERENCES

1. Roth GA, Mensah GA, Johnson CO, et al. Global burden of cardiovascular diseases and risk factors, 1990-2019: update from the GBD 2019 study. *J Am Coll Cardiol*. 2020;76:2982-3021.

2. Ridker PM. Residual inflammatory risk: addressing the obverse side of the atherosclerosis prevention coin. *Eur Heart J*. 2016;37:1720-1722.

3. Perzborn E, Roehrig S, Straub A, Kubitza D, Misselwitz F. The discovery and development of rivaroxaban, an oral, direct factor xa inhibitor. *Nat Rev Drug Discov*. 2011;10:61-75.

4. Patel MR, Mahaffey KW, Garg J, et al. Rivaroxaban versus warfarin in nonvalvular atrial fibrillation. *N Engl J Med*. 2011;365:883-891.

5. Kakkar AK, Brenner B, Dahl OE, et al. Extended duration rivaroxaban versus short-term enoxaparin for the prevention of venous thromboembolism after total hip arthroplasty: a double-blind, randomised controlled trial. *Lancet*. 2008;372:31-39.

6. Eriksson BI, Borris LC, Friedman RJ, et al. Rivaroxaban versus enoxaparin for thromboprophylaxis after hip arthroplasty. *N Engl J Med*. 2008;358:2765-2775.

7. Lassen MR, Ageno W, Borris LC, et al. Rivaroxaban versus enoxaparin for thromboprophylaxis after total knee arthroplasty. *N Engl J Med*. 2008;358:2776-2786.

8. Turpie AG, Lassen MR, Davidson BL, et al. Rivaroxaban versus enoxaparin for thromboprophylaxis after total knee arthroplasty (record4): a randomised trial. *Lancet*. 2009;373:1673-1680.

9. Bauersachs R, Berkowitz SD, Brenner B, et al. Oral rivaroxaban for symptomatic venous thromboembolism. *N Engl J Med*. 2010;363:2499-2510.

10. Mega JL, Braunwald E, Wiviott SD, et al. Rivaroxaban in patients with a recent acute coronary syndrome. *N Engl J Med*. 2012;366:9-19.

11. Eikelboom JW, Connolly SJ, Bosch J, et al. Rivaroxaban with or without aspirin in stable cardiovascular disease. *N Engl J Med*. 2017;377:1319-1330.

12. Hara T, Fukuda D, Tanaka K, et al. Rivaroxaban, a novel oral anticoagulant, attenuates atherosclerotic plaque progression and destabilization in apoe-deficient mice. *Atherosclerosis*. 2015;242:639-646.

13. Posthuma JJ, Posma JJN, van Oerle R, et al. Targeting coagulation factor Xa promotes regression of advanced atherosclerosis in apolipoprotein-e deficient mice. *Sci Rep*. 2019;9:3909.

14. Liu J, Nishida M, Inui H, et al. Rivaroxaban suppresses the progression of ischemic cardiomyopathy in a murine model of diet-induced myocardial infarction. *J Atheroscler Thromb*. 2019;26:915-930.

15. Nystedt S, Emilsson K, Wahlestedt C, Sundelin J. Molecular cloning of a potential proteinase activated receptor. *Proc Natl Acad Sci U S A*. 1994;91:9208-9212.

16. Bono F, Schaeffer P, Hérault JP, et al. Factor xa activates endothelial cells by a receptor cascade between epr-1 and par-2. *Arterioscler Thromb Vasc Biol*. 2000;20:E107-E112.

17. Badeanlou L, Furlan-Freguia C, Yang G, Ruf W, Samad F. Tissue factor-protease-activated receptor 2 signaling promotes diet-induced obesity and adipose inflammation. *Nat Med*. 2011;17:1490-1497.

18. Jiang X, Zhu S, Panetti TS, Bromberg ME. Formation of tissue factor-factor viia-factor xa complex induces activation of the motor pathway which regulates migration of human breast cancer cells. *Thromb Haemost*. 2008;100:127-133.

19. Sandberg WJ, Halvorsen B, Yndestad A, et al. Inflammatory interaction between light and proteinase-activated receptor-2 in endothelial cells: potential role in atherogenesis. *Circ Res*. 2009;104:60-68.

20. Hara T, Phuong PT, Fukuda D, et al. Protease-activated receptor-2 plays a critical role in vascular inflammation and atherosclerosis in apolipoprotein e-deficient mice. *Circulation*. 2018;138:1706-1719.

21. Liao X, Sluimer JC, Wang Y, et al. Macrophage autophagy plays a protective role in advanced atherosclerosis. *Cell Metab*. 2012;15:545-553.

22. Razani B, Feng C, Coleman T, et al. Autophagy links inflammasomes to atherosclerotic progression. *Cell Metab*. 2012;15:534-544.

23. Sciarretta S, Maejima Y, Zablocki D, Sadoshima J. The role of autophagy in the heart. *Annu Rev Physiol*. 2018;80:1-26.

24. Tsuboyama K, Koyama-Honda I, Sakamaki Y, Koike M, Morishita H, Mizushima N. The Atg conjugation systems are important for degradation of the inner autophagosomal membrane. *Science*. 2016;354:1036-1041.

25. Duewell P, Kono H, Rayner KJ, et al. Nlrp3 inflammasomes are required for atherogenesis and activated by cholesterol crystals. *Nature*. 2010;464:1357-1361.

26. Kimura T, Jain A, Choi SW, et al. Trim-mediated precision autophagy targets cytoplasmic regulators of innate immunity. *J Cell Biol*. 2015;210:973-989.

27. Zhou Q, Bea F, Preusch M, et al. Evaluation of plaque stability of advanced atherosclerotic lesions in apo e-deficient mice after treatment with the oral factor xa inhibitor rivaroxaban. *Mediators Inflamm*. 2011;2011:432080.

28. Kubitza D, Becka M, Voith B, Zuehlsdorf M, Wensing G. Safety, pharmacodynamics, and pharmacokinetics of single doses of bay 59-7939, an oral, direct factor xa inhibitor. *Clin Pharmacol Ther*. 2005;78:412-421.

29. Bohm A, Flosser A, Ermler S, et al. Factor-xa-induced mitogenesis and migration require sphingosine kinase activity and s1p formation in human vascular smooth muscle cells. *Cardiovasc Res*. 2013;99:505-513.

30. Osterud B, Lindahl U, Seljelid R. Macrophages produce blood coagulation factors. *FEBS Lett*. 1980;120:41-43.

31. Chen KD, Wang CC, Tsai MC, et al. Interconnections between autophagy and the coagulation cascade in hepatocellular carcinoma. *Cell Death Dis*. 2014;5:e1244.

32. Yan Y, Jiang W, Liu L, et al. Dopamine controls systemic inflammation through inhibition of NLRP3 inflammasome. *Cell*. 2015;160:62-73.

33. Ridker PM, Everett BM, Thuren T, et al. Antiinflammatory therapy with canakinumab for atherosclerotic disease. *N Engl J Med*. 2017;377:1119-1131.

34. Nidorf SM, Fiolet AT, Mosterd A, et al. Colchicine in patients with chronic coronary disease. *N Engl J Med*. 2020;383:1838-1847.

35. Petzold T, Thienel M, Dannenberg L, et al. Rivaroxaban reduces arterial thrombosis by inhibition of fxa-driven platelet activation via protease activated receptor-1. *Circ Res*. 2020;126:486-500.

36. Nording HM, Seizer P, Langer HF. Platelets in inflammation and atherogenesis. *Front Immunol*. 2015;6:98.

37. Yasuda S, Kaikita K, Akao M, et al. Antithrombotic therapy for atrial fibrillation with stable coronary disease. *N Engl J Med*. 2019;381:1103-1113.

KEY WORDS atherosclerosis, autophagy, factor Xa, inflammasome, rivaroxaban

APPENDIX For supplemental figures, please see the online version of this paper.